PROCEEDINGS OF THE SOCIETY FOR EXPERIMENTAL BIOLOGY AND MEDICINE **181**, 41–48 (1986)

Cytophotometric Analysis of Neuronal Chromatin and RNA Changes in Oxotremorine-Treated Rats (42222)

LEE J. MARTIN, JEFFREY A. DOEBLER, AND ADAM ANTHONY

Department of Biology, The Pennsylvania State University, University Park, Pennsylvania 16802

Abstract. Neuronal nucleic acid responses were examined within the rat striatum and sensorimotor cortex (layer V) following single intraperitoneal injections of the central cholinergic–muscarinic agonist oxotremorine (0.1, 0.7, or 1.0 mg/kg). After stoichiometric Feulgen and azure B staining of brain sections, scanning–integrating microdensitometry was used to quantify Feulgen-deoxyribonucleic acid levels, changes in the susceptibility of chromatin to Feulgen acid hydrolysis (F-DNA yield) and azure B-ribonucleic acid (RNA) content of neurons on an individual basis. Changes in neuronal nuclear and nucleolar volumes were also determined histometrically. Within the striatum and sensorimotor cortex, oxotremorine produced marked dose-dependent elevations in both F-DNA yield and RNA content. These metabolic increases were typically paralleled by elevations in nuclear and nucleolar volumes. The data demonstrate that the oxotremorine-induced central muscarinic activation is associated with dose-related enhancements in neuronal chromatin template activity, RNA content, and protein synthetic capacity.

Oxotremorine (OXO), a potent and specific central muscarinic-acetylcholine receptor agonist, produces tremor and rigidity by its actions on the basal ganglia and other brain regions involved with motor function (1, 2). OXO-induced central nervous system stimulation is associated with dose-related elevations in glucose uptake and utilization throughout the entire extrapyramidal system and cerebral cortex (2, 3). However, effects of OXO on other aspects of neuronal metabolism, such as nucleic acid metabolism, have not been previously ascertained. It is well known that among the earliest events associated with increased cellular metabolic activity are marked alterations in chromatin conformation which reflect the transformation of inactive chromatin into transcriptionally active DNA templates for RNA synthesis (4–6). Moreover, it has been reported that synaptic activation of neurons leads first to specific RNA production and this, in turn, to protein synthesis (7–9). Therefore, the current study was undertaken to examine dose-dependent effects of OXO-induced central muscarinic stimulation on neuronal nucleic acid metabolism in rats. Changes in the physicochemical properties of nuclear chromatin and in perikaryal RNA levels within neurons of the striatum and sensorimotor cortex (layer V) were quantified using cytophotometric analyses of Feulgen-DNA (F-DNA) and azure B-RNA stained brain sections. These two brain regions were selected since they have an important role in motor functioning; layer V of the cerebral cortex was specifically analyzed because it is reported to have a large density of high affinity muscarinic binding sites in comparison to other layers (3). In addition, correlative histometric observations were made on changes in neuronal nuclear and nucleolar volumes.

Materials and Methods. Male Sprague–Dawley rats (Hilltop Labs) weighing 275–325 g were randomly assigned into four treatment groups with six per group. Of these, one group served as controls and received single ip injections of 0.9% saline. The remaining three groups were pretreated with atropine methylbromide (1.0 mg/kg, sc; Sigma) 20 min prior to single ip injections of OXO (Sigma) at dosages of either 0.1, 0.7, or 1.0 mg/kg. The purpose of the atropine methylbromide pretreatment was to block peripheral muscarinic effects of OXO. This dosage of atropine methylbromide prevents lacrimation and diarrhea but not tremor in rats treated with 0.1, 0.7, and 1.0 mg/kg OXO (3). All compounds were prepared in 0.9% saline and injected in a final volume of 0.5 ml/kg body wt. Since numerous reports have shown that chemically and/or electrically induced neuronal nucleic acid changes are consistent and reproducible within

0037-9727/86 $1.50

a 1- to 4-hr time interval (7, 8, 10, 11), all animals were killed by decapitation without anesthesia at 2 hr after their final injection. Brains were removed without delay (ca. 3–5 min) and sliced sagittally at the level of the optic chiasm. Coronally sliced segments of the frontal lobe of the right cerebral hemisphere were fixed in Carnoy fixative for subsequent nucleic acid analyses.

Procedures used in cytophotometric DNA and RNA analyses were as described previously (6, 10–12). Briefly, 15-μm paraffin sections were stained for DNA with the Feulgen nucleal reaction (13) and for RNA with azure B (14). Specificity of RNA staining was confirmed using control sections treated with RNase with and without DNase prior to azure B or Feulgen staining. Preliminary studies revealed that neuronal nuclei from control and OXO-treated rats exhibited similar F-DNA hydrolysis patterns over a 5- to 60-min hydrolysis interval. The standard procedure adopted for comparative DNA analysis of neuronal nuclei was a 30-min hydrolysis duration in 3.5 *N* HCl at 37°C (13).

Cytophotometric analyses of F-DNA reactivity and perikaryal RNA content were made using a Vickers M85a scanning–integrating microdensitometer (Vickers Instruments, Malden, Mass.) as described previously (6, 10). A field delimiting mask was employed to isolate individual and entire neurons or nuclei being analyzed. Fixed delimiting mask apertures of 201 and 314 μm^2 were used for F-DNA and azure B-RNA quantification, respectively. To standardize measurements, cytophotometric readings were made on morphometrically homogenous populations of neurons in the striatum (caudate nucleus plus putamen) and cerebral cortex (layer V). Care was exercised to avoid cut or overlapping neurons or nuclei by up and down focusing and using only neurons or nuclei lying in the midfocal plane of the section. It was ascertained that the extent of error in F-DNA and RNA measurements attributable to differences in section thickness (<2%) or to instrument performance (<1%) is negligible relative to the normal extent of variability in F-DNA yield (ca. 11%) and in RNA contents (ca. 24%) of homogenous populations of brain neurons. The general protocol entailed making 10–25 individual measures in the striatum and cerebral cortex for F-DNA and RNA levels from each animal.

Measurements of nuclear and nucleolar diameter were made on azure B stained sections using an ocular micrometer at ×1000. Nuclear volumes were calculated from $V = \pi/6ab^2$ where a = diameter of major axis and b = diameter of minor axis; nucleolar volumes were calculated from $V = \pi/6D^3$ where D = nucleolar diameter (15).

Statistical analyses of data were performed using analysis of variance, Duncan's new multiple range test and the heterogenous χ^2 test. When the analysis of variance F test revealed significant differences between group means, the data were further analyzed using Duncan's test. In addition, individual F-DNA and RNA values were examined in conventional frequency distribution profile form. Histograms were constructed to demonstrate the frequency of occurrence of nuclei and neurons containing low, moderate, and high F-DNA and RNA levels, with the moderate category arbitrarily designated as that portion of the neuronal population where individual F-DNA and RNA values fall within the range of control mean ± 1.0 standard deviation; low and high F-DNA and RNA categories thus represent neurons with measured values for these cytochemical parameters which were less or greater than one deviation from the respective control mean value. Differences among distribution profiles were then compared using the heterogeneous χ^2 test. In all analyses, probabilities of 5% were interpreted as statistically significant.

Results and Discussion. Mean values of nuclear F-DNA reactivity and perikaryal RNA content are shown in Table I; frequency distribution profiles, constructed on the basis of saline-control mean and standard deviation, demonstrating shifts in the relative abundance of nuclei or neurons containing low, moderate, and high F-DNA and RNA levels are depicted in Figs. 1 and 2. Correlative histometric observations showing changes in neuronal nuclear and nucleolar volumes are presented in Table II. Also, representative micrographs of both Feulgen and azure B stained brain sections from control and 1.0 mg/kg OXO-treated rats are exemplified in Fig. 3.

Within the striatum (CP), OXO-induced central muscarinic stimulation produced dose-

TABLE I. EFFECTS OF OXOTREMORINE-INDUCED CENTRAL MUSCARINIC STIMULATION ON STRIATAL AND CEREBROCORTICAL NEURON FEULGEN-DNA REACTIVITY AND RNA CONTENTS

Treatment	Striatum	Cerebral cortex
	F-DNA yield	
Control	80.2 ± 11.8[d]	82.4 ± 10.1[c]
0.1 mg/kg OXO	84.3 ± 5.7[c]	84.7 ± 4.5[b]
0.7 mg/kg OXO	88.0 ± 5.8[b]	87.3 ± 6.3[a]
1.0 mg/kg OXO	90.7 ± 3.4[a]	88.9 ± 5.0[a]
	Neuronal RNA	
Control	89.8 ± 17.5[d]	123.9 ± 30.3[d]
0.1 mg/kg OXO	109.9 ± 20.1[c]	155.5 ± 33.2[c]
0.7 mg/kg OXO	121.5 ± 18.7[b]	175.9 ± 35.2[b]
1.0 mg/kg OXO	133.7 ± 23.8[a]	214.6 ± 47.6[a]

Note. F-DNA yield and RNA content in absorbancy units ± SD. Each value represents the average of 100 individual cytophotometric measurements with 6 rats per group. Means ranked (*a–d*), the highest value designated as (*a*). Means not designated with same superscript are significantly different, $P < 0.05$, Duncan's new multiple range test.

dependent elevations in both nuclear F-DNA yield and neuronal RNA content. This is apparent in the significant ($P < 0.05$) increases in mean F-DNA reactivity and perikaryal RNA levels (Table I), in the marked increases in the frequency occurrence of both high F-DNA yielding nuclei and high RNA containing neurons (Figs. 1, 2), and in the concomitant reductions in low F-DNA and RNA categories. Significant increases in average CP neuron F-DNA reactivity ranged from 5% with 0.1 mg/kg OXO to 13% with 1.0 mg/kg OXO, whereas elevations in mean CP neuron RNA ranged from 22% with the lowest dose of OXO to 49% with the highest OXO dosage (Table I). Moreover, with 1.0 mg/kg OXO, there was a greater than three-fold shift in the relative abundance of neuronal nuclei exhibiting high F-DNA levels and a striking ca. six-fold elevation in the frequency occurrence of high RNA containing perikarya (Figs. 1, 2). Correspondingly, significant ($P < 0.05$) changes in CP neuron nuclear and nucleolar volumes were manifested by ca. 40% and three-fold increases in nuclear and nucleolar volumes, respectively, with the two higher dosages of OXO (Table II).

Within cerebrocortical neurons, OXO treatment eventuated in virtually identical dose-dependent augmentations in chromatin activation and RNA synthesis (Tables I, II; Figs. 1, 2). However, some essential differences exist regarding the magnitude of the increases. For example, cerebrocortical neuron RNA levels were elevated 42 and 72% with 0.7 and 1.0 mg/kg OXO, respectively, despite the slightly lower increases in F-DNA reactivity relative to CP neurons (Table I). Moreover, elevations in cerebrocortical mean nuclear volume were of greater magnitude in comparison to CP neurons, but changes in nucleolar volumes were similar (Table II).

The present study demonstrates that sys-

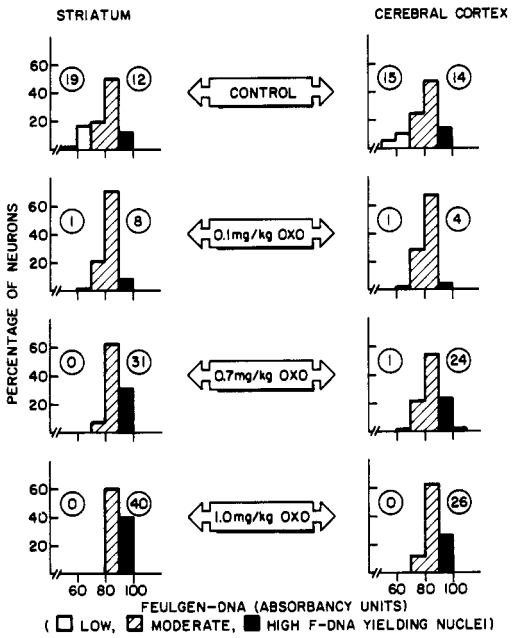

FIG. 1. Frequency distribution profiles depicting dose-dependent alterations in chromatin Feulgen-DNA (F-DNA) reactivity. Histograms were constructed to demonstrate the frequency occurrence of neurons exhibiting low, moderate, and high F-DNA reactivity, the moderate category representing that portion of the neuronal population where individual F-DNA yields fall within ± one standard deviation of saline control mean value. Circled numbers indicate percentages of corresponding low or high F-DNA neurons. Reproducibility of individual nuclear DNA measurements was ±2%. The general protocol entailed making 10–25 individual measures in the striatum and cerebral cortex for F-DNA from each of the six animals in each treatment group.

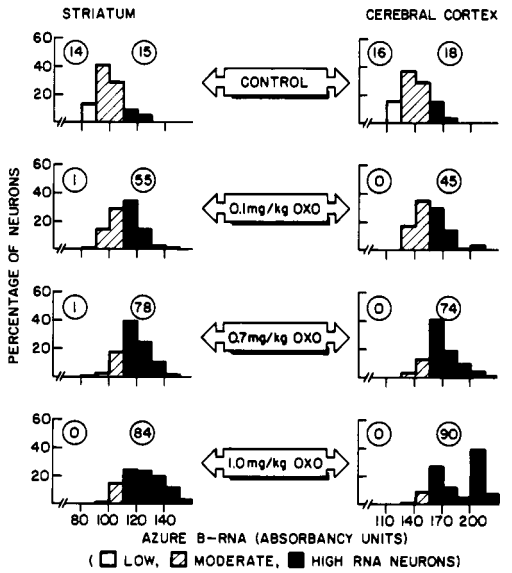

FIG. 2. Frequency distribution profiles of neuronal azure B-RNA contents in oxotremorine-treated rats. Oxotremorine treatment regimen and RNA analyses for each of the six animals per group are described in text. Histograms were constructed to demonstrate the frequency occurrence of neurons containing low, moderate, and high RNA levels, with the moderate category representing that portion of the neuronal population where individual RNA values fall within ± one standard deviation of the control mean value. Circled numbers indicate percentages of low or high RNA containing neurons.

temic treatment with OXO increases, in a dose-related manner, chromatin template activity, and RNA content within neurons of the rat striatum and cerebral cortex (layer V). Our analytical approach involved the use of stoichiometric staining procedures followed by cytophotometric measurement of changes in nuclear F-DNA reactivity and perikaryal RNA on an individual neuron basis. Recent studies have shown that the Feulgen nucleal reaction, which is used mainly for measuring nuclear DNA content and shifts in ploidy distribution patterns (16), can also be used in demonstrating alterations in the physicochemical state of the deoxyribonucleoprotein (DNP)–chromatin complex (6, 17). The basis for this stems from extensive studies indicating that expansion of the chromatin template is frequently associated with an increase in the acid lability of the DNP–chromatin and hence an increased F-DNA staining. Such a response, which has been designated as the "chromatin activation" reaction (4), is presumed to be indicative of a heightened metabolic state and enhanced chromatin template activity and RNA synthetic capacity. Similarly, the content of perikaryal RNA and nuclear and nucleolar volumes directly relates to the level of nerve cell activity and therefore protein synthetic capability (18–20).

At present it is uncertain whether a direct relationship exists between currently observed OXO-induced elevations in neuronal RNA content and previously reported increases in brain oxidative metabolism. However, since glucose oxidation via the pentose cycle (pentose phosphate pathway or hexose monophosphate shunt) is known to provide a route for synthesis of pentose nucleotides for nucleic acid anabolism (21), the early increase in neuronal glucose utilization in OXO-treated animals may be a prerequisite for enhancements

TABLE II. EFFECTS OF OXOTREMORINE-INDUCED CENTRAL MUSCARINIC STIMULATION ON STRIATAL AND CEREBROCORTICAL NEURON NUCLEAR AND NUCLEOLAR VOLUMES

Treatment	Striatum	Cerebral cortex
	Nuclear volume (μm^3)	
Control	1848.3 ± 347.3[b]	1989.3 ± 318.7[b]
0.1 mg/kg OXO	2329.4 ± 200.0[a,b]	2990.2 ± 381.9[a]
0.7 mg/kg OXO	2651.0 ± 459.3[a]	3459.0 ± 706.0[a]
1.0 mg/kg OXO	2625.0 ± 445.0[a]	3138.7 ± 473.5[a]
	Nucleolar volume (μm^3)	
Control	20.1 ± 9.7[c]	32.9 ± 14.6[c]
0.1 mg/kg OXO	44.3 ± 19.1[b]	63.6 ± 20.5[b]
0.7 mg/kg OXO	61.8 ± 25.4[a]	68.0 ± 22.8[b]
1.0 mg/kg OXO	63.9 ± 20.7[a]	87.9 ± 31.0[a]

Note. Mean values (±SD) of nuclear and nucleolar volumes, as measured in striatal and cerebrocortical neurons (layer V) with an ocular micrometer at ×1000. Measurements of nuclear and nucleolar diameters were made on a minimum of 30 neurons in each group of six animals. Nuclear volume was calculated from the equation $V = \pi/6\ ab^2$, where a = diameter of major axis and b = diameter of minor axis. Nucleolar volume was calculated from the equation $V = \pi/6\ D^3$, where D = nucleolar diameter. Means ranked (a–c), the highest value designated as (a). Means not designated with same superscript are significantly different, $P < 0.05$, Duncan's new multiple range test.

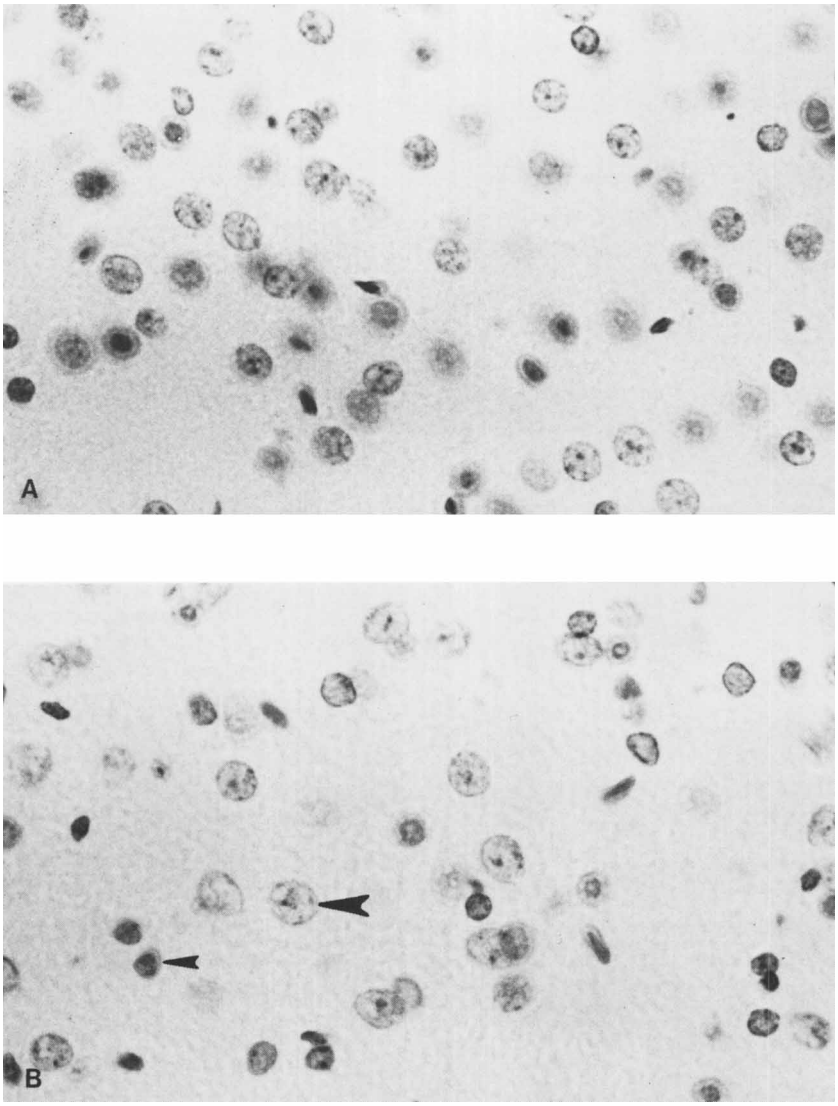

FIG. 3. Representative photomicrographs of Feulgen-DNA (A and B) and azure B-RNA (C and D)-stained cerebrocortical neurons. A and C represent sections from saline control; B and D represent sections from 1.0 mg/kg OXO-treated rat. Note apparent OXO-induced increases in nuclear and nucleolar area (B and D) and in perikaryal RNA content (D). Large arrowheads in B and D indicate a typical nucleus or neuron measured cytophotometrically; small arrowhead in B identifies glial cell. During cytophotometry, care was exercised to avoid cut perikarya and ensure that measured neurons did not overlap in different focal planes. Feulgen-DNA micrographs ×506; azure B-RNA micrographs ×503.

in RNA levels. In highly metabolically active cells, a close relationship does exist between glucose-6-phosphate dehydrogenase activity, a cytochemical marker for pentose cycle activity, and RNA synthesis. For example, in cells undergoing rapid growth and respiration a marked increase in this enzyme is accompanied by augmented RNA production (21). To provide more definitive evidence in this regard, effects of OXO on neuronal glucose-6-phosphate dehydrogenase activity should be examined.

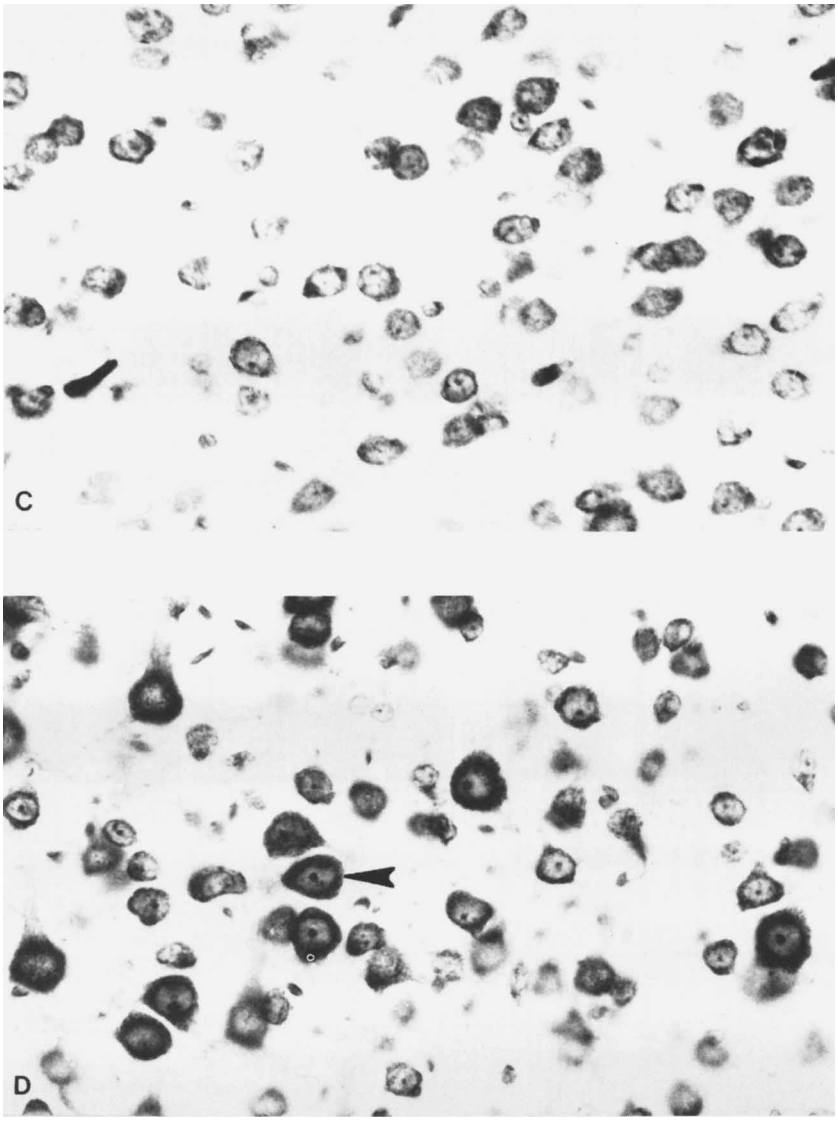

FIG. 3—*Continued.*

An important contribution of the present study is providing further documentation that neuronal RNA content constitutes a very sensitive cytodiagnostic marker of drug-induced changes in neuronal functioning. The successful use of RNA cytophotometry in this and related studies suggests that this approach will have broad applicability in experimental pathology, pharmacology, and neurophysiology. The observation that OXO increases chromatin template activity and RNA content within neurons of the striatum and cerebral cortex may have therapeutic relevance with regard to declines in brain metabolism that occur in aged animals and human Alzheimer's disease. Age-related impairments in CNS metabolism include reductions in neuronal euchromatin to heterochromatin ratios (5), RNA content (19, 20), nuclear and nucleolar volumes (9, 15), and protein synthesis (22, 23).

These metabolic changes have been interpreted as being manifestations of declines in neuronal activation stemming from alterations in various neurotransmitter networks, particularly cholinergic systems (24, 25). Several functionally relevant changes in cholinergic parameters have been identified in aged rodent and Alzheimer's disease brains. These include declines in striatal and cortical choline acetyltransferase (26), acetylcholinesterase (27, 28), and high affinity choline uptake (29). In contrast, the central cholinergic muscarinic receptor remains relatively unaffected (30). Thus, it would be of interest to determine whether OXO-induced central muscarinic activation prevents or mitigates the age-related, neuronal metabolic collapse and thereby increasing the level of functional capacity present in senescent neurons.

This research was supported in part by USAMRDC Contract DAMD 17-81-C-1202.

1. DeFeudis FV. Central Cholinergic Systems and Behavior. New York, Academic Press, p223, 1974.
2. Dow-Edwards D, Dam M, Peterson JM, Rapoport SI, London ED. Effect of oxotremorine on local cerebral glucose utilization in motor system regions of the rat brain. Brain Res **226**:281–289, 1981.
3. Dam M, Wamsley JK, Rapoport SI, London ED. Effects of oxotremorine on local glucose utilization in the rat cerebral cortex. J Neurosci **2**:1072–1078, 1982.
4. Ringertz NR. Cytochemical properties of nuclear proteins and deoxyribonucleoprotein complexes in relation to nuclear function. In: Lima de Faria A, ed. Handbook of Molecular Cytology. Amsterdam, North-Holland, p656, 1969.
5. Crapper DR, Quitkat S, DeBoni U. Altered chromatin conformation in Alzheimer's disease. Brain **102**:483–495, 1979.
6. Anthony A, Hollis TM, Penman JA, Zerweck C, Doebler JA. Feulgen-deoxyribonucleic acid analysis of rabbit aortic smooth muscle cells using scanning-integrating microdensitometry. J Histochem Cytochem **29**:1165–1170, 1981.
7. Hyden H. Cytophysiological aspects of the nucleic acids and proteins in nervous tissue. In: Elliot KAC, Page IH, Quastel JH, eds. Neurochemistry. Springfield: Thomas, p331, 1962.
8. Berry RW. Ribonucleic acid metabolism of a single neuron: correlation with electrical activity. Science (Washington, DC) **166**:1021–1023, 1969.
9. Mann DMA, Yates PO, Barton CM. Cytophotometric mapping of neuronal changes in senile dementia. J Neurol Neurosurg Psychiatry **40**:299–302, 1977.
10. Anthony A, Doebler JA, Bocan TMA, Shih TM. Scanning-integrating microdensitometric analyses of brain neuronal RNA and acetylcholinesterase in acute soman treated rats. Cell Biochem Funct **1**:30–36, 1983.
11. Doebler JA, Bocan TMA, Moore RA, Shih TM, Anthony A. Brain neuronal RNA metabolism during acute soman toxication: Effects of antidotal pretreatments. Neurochem Res **8**:997–1011, 1983.
12. Martin LJ, Doebler JA, Swisher JW, Shih T-M, Anthony A. Scanning cytophotometric analysis of myocardial nucleic acid and chromatin changes in soman toxicated rabbits. Cell Biochem Funct **2**:237–242, 1984.
13. Fand SB. Environmental conditions for optimal Feulgen hydrolysis. In: Wied CL, Bahr BF, eds. Introduction to Quantitative Cytophotometry II. New York, Academic Press, p209, 1970.
14. Shea JR. A method for *in situ* cytophotometric estimation of absolute amount of RNA using azure B. J Histochem Cytochem **18**:143–152, 1970.
15. Mann DMA, Neary D, Yates PO, Lincoln J, Snowden JS, Stanworth P. Alterations in protein synthetic capability of nerve cells in Alzheimer's disease. J Neurol Neurosurg Psychiatry **44**:97–102, 1981.
16. Sandritter W. A review of nucleic acid cytophotometry in general pathology. In: Pattison JR, Bitensky L, Chayen J, eds. Quantitative Cytochemistry and Its Applications. New York, Academic Press, p1, 1979.
17. Kjellstrand PTT. Feulgen acid hydrolysis. Doctoral dissertation, University of Lund, Lund, Sweden, 1976.
18. Watson WE. Observations on the nucleolar and total cell body nucleic acid of injured nerve cells. J Physiol (London) **196**:655–676, 1968.
19. Mann DMA, Yates PO. Lipoprotein pigments—Their relationship to ageing in the human nervous system. I. The lipofuscin content of nerve cells. Brain **97**:481–488, 1974.
20. Mann DMA. Nerve cell protein metabolism and degenerative disease. Neuropathol Appl Neurobiol **8**: 161–176, 1982.
21. Nandy K. Further studies on the effects of centrophenoxine on the lipofuscin pigment in the neurons of senile guinea pigs. J Gerontol **23**:82–92, 1968.
22. Dwyer BE, Fando JL, Wasterlain CC. Rat protein synthesis declines during postdevelopmental aging. J Neurochem **35**:746–749, 1980.
23. Fando JL, Wasterlain CG. Age-dependent changes in brain protein synthesis in the rat. Neurochem Res **5**: 23–33, 1980.
24. Mann DMA, Yates PO, Marcyniuk B. Alzheimer's presenile dementia, senile dementia of the Alzheimer's type and Down's syndrome in middle age form and related continuum of pathological changes. Neuropathol Appl Neurobiol **10**:185–207, 1984.
25. Mann DMA, Yates PO, Marcyniuk B. Changes in nerve cells of the nucleus basalis of Meynert in Al-

zheimer's disease and their relationship to ageing and to the accumulation of lipofuscin pigment. Mech Ageing Dev **25**:189–204, 1984.
26. Davies P. Neurotransmitter-related enzymes in senile dementia of the Alzheimer's type. Brain Res **171**:319–327, 1979.
27. Op den Velde W, Stam FC. Some central proteins in enzyme systems in Alzheimer's presenile and senile dementia. J Amer Geriatr Soc **24**:12–16, 1976.
28. Perry EK, Perry RH, Blessed G, Tomlinson BE. Necropsy evidence of central cholinergic deficit in senile dementia. Lancet **1**:189, 1977.
29. Bowen DM, Davison AM. Changes in brain lysosomal activity, neurotransmitters, related enzymes and other proteins in senile dementia. In: Katzman R, Terry RD, Bicks KL, eds. Alzheimer's Disease, Senile Dementia and Related Disorders. New York, Raven Press, p421, 1978.
30. Davies P, Verth AH. Regional distribution of muscarinic acetylcholine receptors in normal and Alzheimer's type dementia brains. Brain Res **138**:385–392, 1978.

Received April 29, 1985. P.S.E.B.M. 1986, Vol. 181.
Accepted September 4, 1985.